The Influence of Solvent in Controlling Peptide-Surface Interactions

*Daniel A. Cannon,[1] Nurit Ashkenasy,[2] Tell Tuttle[1]**

[1] WestCHEM, Department of Pure and Applied Chemistry University of Strathclyde

295 Cathedral Street, Glasgow G1 1XL (UK)

[2] Department of Materials Engineering and the Ilze Katz Institute for Nanoscale Science and Technology, Ben-Gurion University of the Negev, Beer-Sheva, Israel

AUTHOR INFORMATION

Corresponding Author

*tell.tuttle@strath.ac.uk

Protein binding to surfaces is an important phenomenon in biology and in modern technological applications. Extensive experimental and theoretical research has been focused in recent years on revealing the factors that govern binding affinity to surfaces. Theoretical studies mainly focus on examining the contribution of the individual amino acids or, alternatively, the binding potential energies of the full peptide, which are unable to capture entropic contributions and neglect the dynamic nature of the system. We present here a methodology that involves the combination of non-equilibrium dynamics simulations with strategic mutation of polar residues to reveal the different factors governing the binding free energy of a peptide to a surface. Using a gold binding peptide as an example, we show that relative binding free energies are a consequence of the balance between strong interactions of the peptide with the surface, and the ability for the bulk solvent to stabilize the peptide.

TOC GRAPHIC

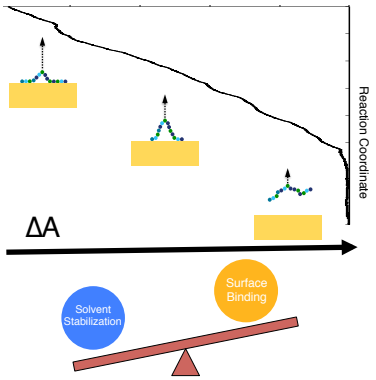

KEYWORDS

Steered Molecular Dynamics, Surface Binding, Peptide-Surface, Solvent Stabilization, Binding Free Energy

Surface-biomolecule interactions have found widespread applicability in the field of nanotechnology. These interactions have been successfully exploited for the synthesis of metal nanoparticles with controlled size[1-4] and surface morphology[5] and for controlling the surface electronic properties of semiconductors.[6] The identification of biopolymers that bind to a particular surface is often achieved through screening techniques such as phage display[7-8] and cell surface display[9-10] (CSD). Both experimental[4, 11-12] and computational[13-18] studies, have focused on the important question of why certain peptide sequences show affinity and specificity for particular metals or crystal architectures. Understanding the different parameters that govern this control remains a challenge, but could ultimately facilitate *de novo* design of surface-selective binding sequences.

One of the most useful sequences is the gold-binding peptide (GBP) (MHGKTQATSGTIQS), known as GBP1, which was discovered from Escherichia coli CSD libraries.[11] GBP1 has been used in the controlled synthesis of gold nanoparticles,[2, 4, 19] boasting excellent regulation of particle size. An investigation of the conformational properties of the 42 residue, 3R-GBP1 (triple repeat of GBP1)[13-14] proposed that binding affinity is an inherent property of the high occurrence of hydroxyl moieties, via serine and threonine side chains. On the other hand, a combined experimental and theoretical study by Tang et al.[15] suggested that three anchoring residues in the N-terminal region of the sequence (M1, H2 and Q6) allow the adsorbed peptide to experience greater conformational freedom resulting in entropically driven binding. In a related work, the binding energy of GBP1 to gold has been derived by considering the binding free energies of the individual amino acids that constitute the peptide and assuming that these remain unchanged *in situ* within the peptide chain.[20] Alternative studies have considered the full peptide structure to calculate binding energy via the compartmentalization method,[21-22] which provides an

indication of the binding potential energy of the peptide through single snapshots of the peptide in the adsorbed and bulk states. However, to provide binding free energies and consider multiple binding modes dynamic methods should be employed.

Recently, non-equilibrium approaches have been successfully utilized to obtain binding free energies of peptides to surfaces from non-equilibrium simulations.[23-24] In particular, Mijajlovic *et al*.[24] have employed non-equilibrium thermodynamic integration[25-26] (NETI) in combination with steered molecular dynamics[27] (SMD) to calculate the Helmholtz free energy of adsorption for a pentapeptide bound to graphene to calculate binding free energies for a number of different potential binding conformations. In the current work we utilize this method to calculate the binding free energy of the tetrakaideca peptide **GBP1** to a gold surface. By applying this approach to a set of substitute-out/substitute-in mutations we show that the stability of the peptide in the bulk solution is critical in determining the binding free energy of the peptide to the gold surface.

To gain a comprehensive insight into the relationship between the sequence and binding strength of GBP1 we use a series of mutations, outlined in Table 1. In this design, the native **GBP1** sequence is compared to its analogous alanine control, **A14**. Furthermore, a substitute-out/substitute-in mutation approach was used for **GBP1** and **A14** respectively, where mutations were based on three categories of amino acid: single heteroatom side chains (M, K) in **GBP1-MK** and **A14+MK**, hydroxyl residues (S, T) in **GBP1-ST** and **A14+ST**, and two heteroatom side chains (H, Q) in **GBP1-HQ** and **A14+HQ** (see Table 1 for nomenclature and complete sequences). This method allows the influence of each amino acid towards peptide-surface binding affinity to be separated into its ability to form strong non-covalent interactions with the surface on the one hand, and its contribution to destabilization of the unbound peptide in solution

on the other, revealing both the contribution of residue binding affinity (in the context of the peptide) and destabilization of the peptide's conformation in solution to the binding free energy of the peptide.

Table 1. Peptide sequences under study. **GBP1** is the native sequence and **A14** is the alanine control. Mutations from native and control sequences are highlighted.

Sequence	1	2	3	4	5	6	7	8	9	10	11	12	13	14
GBP1	M	H	G	K	T	Q	A	T	S	G	T	I	Q	S
GBP1-MK	**A**	H	G	**A**	T	Q	A	T	S	G	T	I	Q	S
GBP1-ST	M	H	G	K	**A**	Q	A	**A**	**A**	G	**A**	I	Q	**A**
GBP1-HQ	M	**A**	G	K	T	**A**	A	T	S	G	T	I	**A**	S
A14	A	A	A	A	A	A	A	A	A	A	A	A	A	A
A14+MK	**M**	A	A	**K**	A	A	A	A	A	A	A	A	A	A
A14+ST	A	A	A	A	**T**	A	A	**T**	**S**	A	**T**	A	A	**S**
A14+HQ	A	**H**	A	A	A	**Q**	A	A	A	A	A	A	**Q**	A

Molecular dynamics (MD) simulations of GBP1 in a periodic box of TIP3P water (see Supporting Information for simulation details) predicted an equilibrated structure with two distinct regions (Figure 1a), with the N-terminal region (MHGKTQA) adopting a coiled structure while residues 8 to 14 of the peptide (TSGTIQS) adopt an extended conformation, the chemical structure of which is shown in Figure 1b. This structure is consistent with the available NMR data for this sequence,[28] thus validating the ability for the methods employed to predict physically stable structures of the peptide.

a)

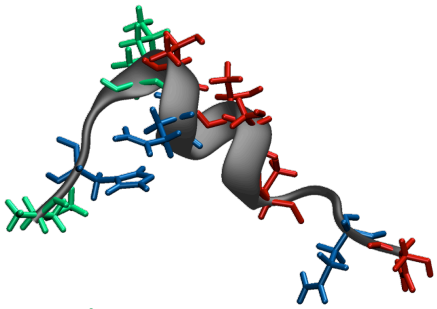

b)

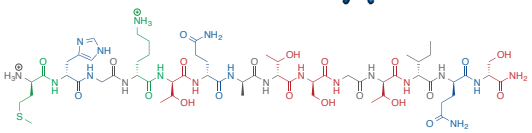

Figure 1. a) Final structure of GBP1 after a 20 ns equilibration simulation in TIP3P solvent with periodic boundary conditions (see Supporting Information for simulation details). b) Full chemical structure of sequence **GBP1**, M/K residues are shown in green, S/T in red and H/Q in blue.

The peptide, in its final conformation from the equilibration simulation, was placed at six different orientations above the metal surface in order to avoid bias between configuration and adsorption behavior (Figure S2, Supplementary Information). The peptide was allowed to adsorb to the Au (111) surface over a period of 70 ns from each starting configuration. All simulations were carried out at 300 K in the NAMD 2.8[29] molecular dynamics package, employing the CHARMM-METAL[30] force field to describe the gold, CHARMM22[31] for the peptides and the TIP3P[32] model for water potentials. The peptide was considered to be adsorbed if the center of mass was within 4.5 Å of the metal surface. Above this cut-off, binding energies were found to differ significantly and thus did not represent adsorbed states of the system. The same adsorption protocol was employed for all sequences and using this criteria, it was found that for each mutation, at least four starting configurations adsorbed to the surface. The center of mass for the

adsorbed peptides that were used in the subsequent desorption simulations varied between 3.30 Å and 4.50 Å from the surface (see Table S1 in the Supporting Information for details). Complete details of the system setup can be found in the Supporting Information. Examination of the adsorbed structures indicated that the peptide prefers to orientate such that the heteroatoms are situated in the space between atoms in the top Au layer of the surface, above the atoms of the second layer (see Figures S3 – S10 in the Supporting Information for the final snapshots of each adsorbed structure). Furthermore, the alignment of the polar groups, especially glutamine, coincides well with the soft-epitaxial mode of adsorption, which has been observed previously,[21, 33] where the Au (111) surface geometry creates binding sites for polar side chains.

The binding free energy was derived from the work required to pull the peptide from the adsorbed state through Jarzynski's equality, equation 1.[25-26, 34]

$$\Delta A = -k_B T * ln\langle e^{-W/k_B T}\rangle \quad (1)$$

Where ΔA is the Helmholtz free energy, k_B is the Boltzmann constant, T is temperature, and W is the work. The combined NETI-SMD approach was used to calculate the equilibrium free energies from multiple short non-equilibrium simulations, in conjunction with statistical bootstrapping of multiple simulations to increase accuracy. An important feature of our methodology is that free energy calculations were performed on the peptide sequence in its entirety, as opposed to the combination of single amino acids, hence the impact of each type of residue on binding strength was measured in the context of its native peptide environment. Thirty desorption simulations were performed for each adsorbed conformation, giving between 120 and 180 simulations per sequence. A harmonic constraint of 500 kcal mol^{-1} $Å^{-1}$ was applied to the C_α of residue 7 of the peptide, which was pulled at a constant rate of 0.005 Å/ps from the gold (*x*y)

plane. The resulting free energy curve for the native peptide, **GBP1**, is shown as an example in Figure 2a.

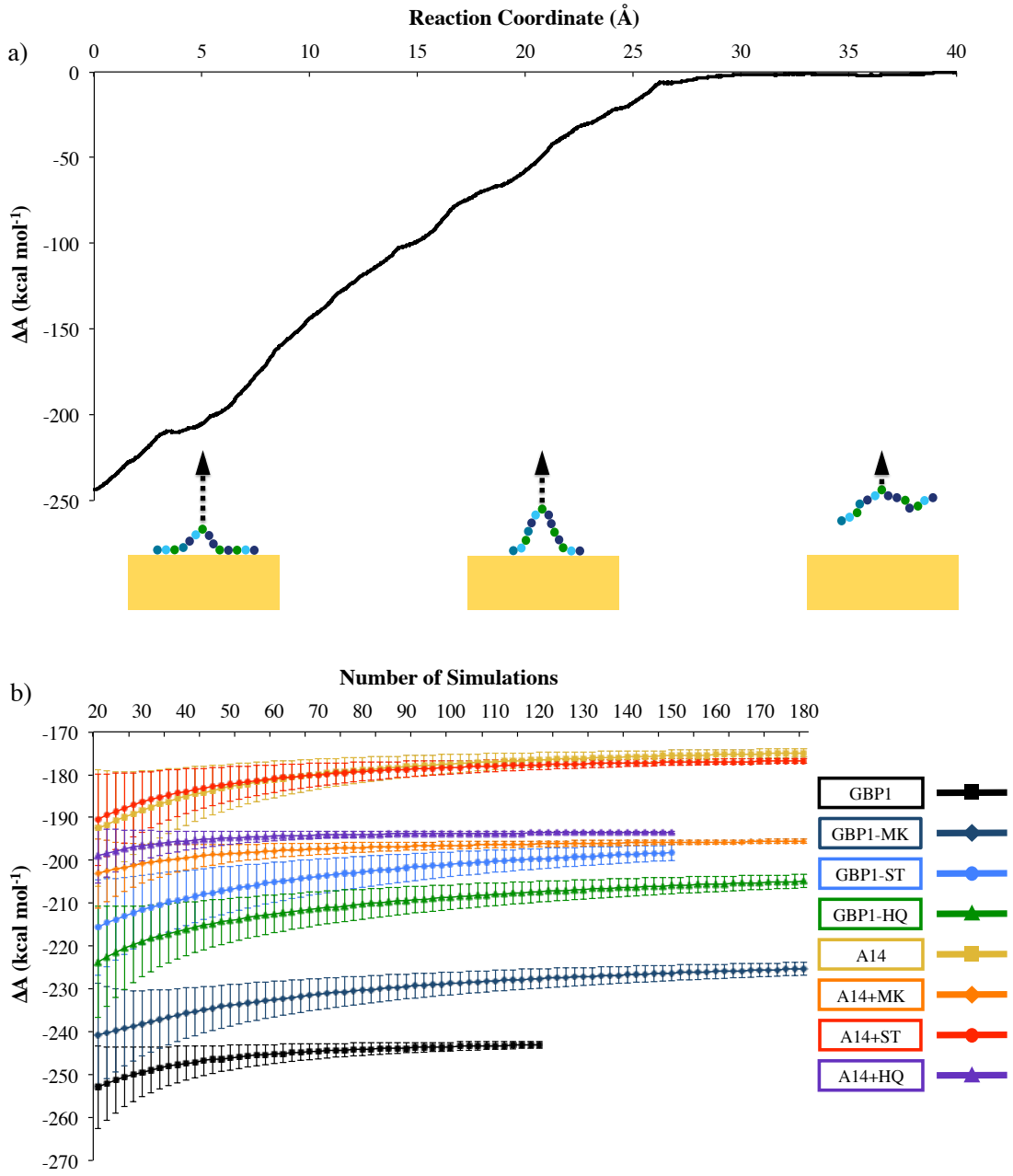

Figure 2. a) The change in binding free energy, ΔA, plotted as a function of desorption reaction coordinate for **GBP1**. The desorption process is depicted at the bottom of the graph. b) Change

in ΔA as a function of the number of simulations used in the bootstrapping analysis for all adsorbed conformations of the different peptides.

The convergence of binding free energy as a function of the number of simulations used in the bootstrapping analysis is shown in Figure 2b, we defined ΔA as being converged when the associated errors were less than ± 2.0 kcal mol^{-1}.

Table 2. Binding free energies, ΔA, for sequences **GBP1** to **A14+HQ**.

Sequence	ΔA (kcal mol^{-1})
GBP1	-243.0
GBP1-MK	-225.3
GBP1-ST	-198.2
GBP1-HQ	-204.8
A14	-174.9
A14+MK	-195.5
A14+ST	-176.8
A14+HQ	-193.5

ΔA values reported herein are the difference between the adsorbed state at 0 Å and the bulk state at 40 Å. The binding free energies for all eight sequences are shown in Table 2. As expected, the native **GBP1** sequence shows the greatest binding free energy (ΔA_{GBP1} = -243.0 kcal mol^{-1}) and the alanine control **A14** shows the weakest binding (ΔA_{A14} = -174.9 kcal mol^{-1}). Upon substitution of M1 and K4 for alanine (**GBP1-MK**) a loss in binding strength of +17.7 kcal mol^{-1} is observed, representing a loss of approximately +8.9 kcal mol^{-1} per residue. Mutation of the control sequence to include methionine and lysine (**A14+MK**) shows a recovery in binding strength of -20.6 kcal mol^{-1} (-10.3 kcal mol^{-1} per residue) similar to the loss of the corresponding **GBP1-MK** mutation. A loss in binding free energy of +9.0 kcal mol^{-1} per residue was found for the mutation of hydroxyl amino acids ($\Delta\Delta A_{GBP1/GBP1-ST}$ = +44.8 kcal mol^{-1}); however the

introduction of hydroxyl moieties in sequence **A14+ST** does not yield any significant increase in binding strength over the control sequence **A14** (ΔA_{A14} = -174.9 kcal mol^{-1}, ΔA_{A14+ST} = -176.8 kcal mol^{-1}). A similar discrepancy is observed for the mutation of histidine and glutamine residues **GBP1-HQ**, where the loss of +38.2 kcal mol^{-1} (+12.7 kcal mol^{-1} per residue) upon removal from the native sequence is more substantial than the gain of -18.6 kcal mol^{-1} in binding free energy strength when replacing alanine in the control, (**A14+HQ**).

If the binding strength were governed by interaction strength of the single amino acids with the gold surface, the loss observed in substitute-out mutations would be equivalent to the gain in corresponding substitute-in sequences. Hence, these results demonstrate that binding strength is not influenced solely, or even predominantly, by the affinity that individual amino acids have for the Au (111) surface. This phenomena can be explained by changes in the stability of the peptide in the water environment upon sequence mutation in addition to the loss of anchoring points between the peptide and gold. For example, replacing polar residues for non-polar alanine in the substitute-out mutations reduces the ability of the peptide to stabilize interactions with water in the bulk solution, hence it is more favorable for the peptide to remain on the surface, enhancing binding strength. Conversely, introduction of polar residues in the substitute-in mutations stabilizes the peptide in the water bulk and consequently decreases the binding strength. The significance of this effect is clearly dependent on the nature of the entire peptide.

The effects of the nature of residues on the conformation of the peptide in the bulk water are clearly observed in Figure 3. **GBP1-ST** retains the coiled character of the **GBP1** peptide, while **A14+ST** adopts a more open conformation; consequently serine and threonine residues can more readily form stabilizing interactions with water, meaning that binding between the peptide and the surface is almost completely diminished due to its affinity for the bulk ($\Delta\Delta A_{A14/A14+ST}$ = -1.9

kcal mol^{-1}). In general, sequences with hydroxyl side chains appear to promote the unwinding of the characteristic coiled structure of GBP1 (Figure 3 b, d and g), indicating stabilization of the peptide in the bulk water. Figures 3a, c and h show that sequences containing histidine and glutamine retain coiled character, suggesting that in these mutations the peptide would more readily adsorb on the surface as the peptide overall is destabilized in the bulk compared to the open structures containing serine and threonine. Indeed, sequence **A14+HQ** (Figure 3 g), which preferentially forms a coil in solution, gives only a partial loss in binding free energy relative to **GBP1-HQ** ($\Delta\Delta A_{GBP1/GBP1\text{-}HQ}$ = +38.2 kcal mol^{-1} $\Delta\Delta A_{A14/A14+HQ}$ = -18.6 kcal mol^{-1}) as a result of less favorable interactions with the bulk water.

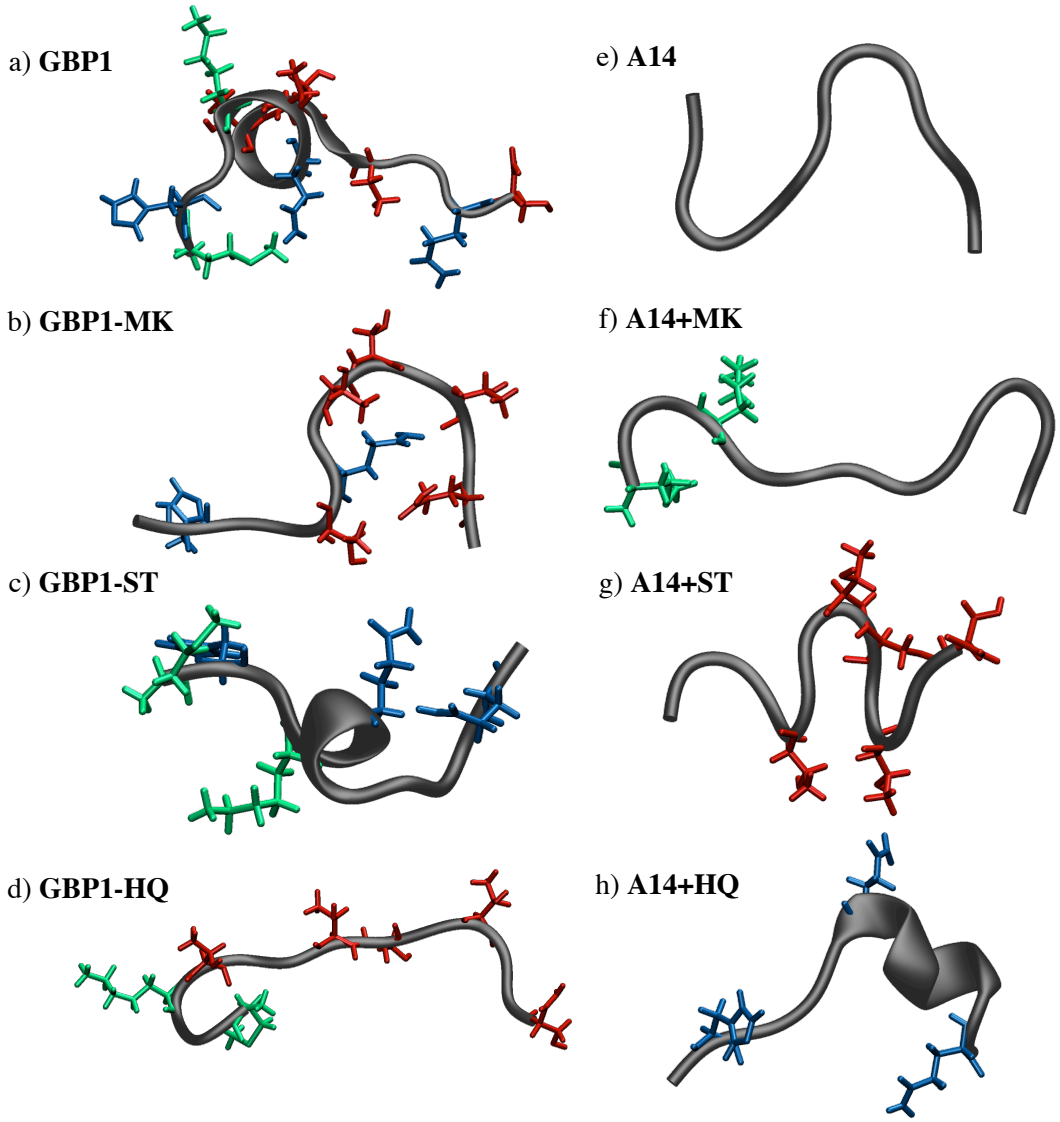

Figure 3. Structures of sequences **GBP1** and its three mutations (a – d) and **A14** control and its mutations (e – h) after 20 ns equilibration in water. Residues involved in mutations are shown explicitly: M/K shown in green, S/T in red and H/Q in blue.

Unlike the coiled structure of **GBP1** (Figure 3a) the alanine control, **A14** (Figure 3e) shows no indication of secondary structure formation. Particularly interesting is the final structure at the completion of the 20 ns simulation of **GBP1-MK** (Figure 3b), where the presence of both H, Q and hydroxyl moieties results in both a loss of coil and a closing of the peptide from positions 5

to 14. This may suggest a clash between the solvent stabilizing effects of S and T and the promotion of a closed structure by histidine and glutamine. The contribution of methionine and lysine remains almost equivalent for the substitute out (Figure 3b), substitute in (Figure 3f) mutations, ($\Delta\Delta A_{GBP1/GBP1\text{-}MK}$ = +17.7 kcal mol^{-1} $\Delta\Delta A_{A14/A14+MK}$ = -20.6 kcal mol^{-1}), regardless of peptide environment, indicating that for these residues binding free energy is almost entirely a result of side chain interactions with the solid surface and do not significantly alter peptide stability in water.

In conclusion, by employing a substitute-in/substitute-out mutation approach, we reveal that the binding strength of peptides to surfaces is a delicate balance between the interactions of the peptide with both the surface and the aqueous solvent. In particular, the combination of strategic mutation and non-equilibrium molecular dynamics protocols reveals that both peptide gold interactions and the stability in solvent shape **GPB1** binding to gold, for which we have found that methionine and lysine contribute approximately -8.9 kcal mol^{-1}, serine and threonine -9.0 kcal mol^{-1} and histidine and glutamine -12.7 kcal mol^{-1} per residue to the binding character.

ASSOCIATED CONTENT

Supporting Information.

Detailed information on simulation setup can be found in the Supporting Information along with adsorbed peptide center of mass distances and the structures of adsorbed peptides on the gold surface. This material is available free of charge via the Internet at http://pubs.acs.org.

AUTHOR INFORMATION

Corresponding Author

*tell.tuttle@strath.ac.uk

ACKNOWLEDGMENT

The authors acknowledge ARCHIE-WeSt High Performance Computing facilities where all calculations discussed in the paper were performed. We also acknowledge Dr. Milan Mijajlovic and Prof. Mark J. Biggs of the University of Adelaide for useful discussions regarding statistical bootstrapping and provision of related scripts. This research was supported by the Israel Science Foundation (grant No. 1519/14)

REFERENCES

(1) Naik, R. R.; Stringer, S. J.; Agarwal, G.; Jones, S. E.; Stone, M. O. Biomimetic Synthesis and Patterning of Silver Nanoparticles *Nat. Mater.,* **2002,** *1*, 169-172, 10.1038/nmat758

(2) Wang, Z.; Chen, J.; Yang, P.; Yang, W. Biomimetic Synthesis of Gold Nanoparticles and Their Aggregates Using a Polypeptide Sequence *Appl. Organomet. Chem.,* **2007,** *21*, 645-651, 10.1002/aoc.1222

(3) Sarikaya, M.; Tamerler, C.; Jen, A. K. Y.; Schulten, K.; Baneyx, F. Molecular Biomimetics: Nanotechnology through Biology *Nat Mater,* **2003,** *2*, 577-585, 10.1038/nmat964

(4) Tamerler, C.; Duman, M.; Oren, E. E.; Gungormus, M.; Xiong, X.; Kacar, T.; Parviz, B. A.; Sarikaya, M. Materials Specificity and Directed Assembly of a Gold-Binding Peptide *Small,* **2006,** *2*, 1372-1378, 10.1002/smll.200600070

(5) Matmor, M.; Ashkenasy, N. Peptide Directed Growth of Gold Films *J. Mater. Chem.,* **2011,** *21*, 968-974, 10.1039/C0JM02343D

(6) Matmor, M.; Ashkenasy, N. Modulating Semiconductor Surface Electronic Properties by Inorganic Peptide–Binders Sequence Design *J. Am. Chem. Soc.,* **2012,** *134*, 20403-20411, 10.1021/ja3078494

(7) Smith, G. P. Filamentous Fusion Phage: Novel Expression Vectors That Display Cloned Antigens on the Virion Surface *Science,* **1985,** *228*, 1315-1317, 10.1126/science.4001944

(8) Kehoe, J. W.; Kay, B. K. Filamentous Phage Display in the New Millennium *Chem. Rev. (Washington, DC, U. S.),* **2005,** *105*, 4056-4072, 10.1021/cr000261r

(9) Georgiou, G.; Stathopoulos, C.; Daugherty, P. S.; Nayak, A. R.; Iverson, B. L.; Iii, R. C. Display of Heterologous Proteins on the Surface of Microorganisms: From the Screening of Combinatorial Libraries to Live Recombinant Vaccines *Nat Biotech,* **1997,** *15*, 29-34, 10.1038/nbt0197-29

(10) Daugherty, P. S. Protein Engineering with Bacterial Display *Curr. Opin. Struct. Biol.,* **2007,** *17*, 474-480, 10.1016/j.sbi.2007.07.004

(11) Brown, S. Metal-Recognition by Repeating Polypeptides *Nat Biotech,* **1997,** *15*, 269-272, 10.1038/nbt0397-269

(12) Wei, Y.; Latour, R. A. Determination of the Adsorption Free Energy for Peptide−Surface Interactions by Spr Spectroscopy *Langmuir,* **2008,** *24*, 6721-6729, 10.1021/la8005772

(13) Braun, R.; Sarikaya, M.; Schulten, K. Genetically Engineered Gold-Binding Polypeptides: Structure Prediction and Molecular Dynamics *J. Biomater. Sci., Polym. Ed.,* **2002,** *13*, 747-757, 10.1163/156856202760197384

(14) Verde, A. V.; Acres, J. M.; Maranas, J. K. Investigating the Specificity of Peptide Adsorption on Gold Using Molecular Dynamics Simulations *Biomacromolecules,* **2009,** *10*, 2118-2128, 10.1021/bm9002464

(15) Tang, Z.; Palafox-Hernandez, J. P.; Law, W.-C.; E. Hughes, Z.; Swihart, M. T.; Prasad, P. N.; Knecht, M. R.; Walsh, T. R. Biomolecular Recognition Principles for Bionanocombinatorics: An Integrated Approach to Elucidate Enthalpic and Entropic Factors *ACS Nano,* **2013,** *7*, 9632-9646, 10.1021/nn404427y

(16) Palafox-Hernandez, J. P.; Tang, Z.; Hughes, Z. E.; Li, Y.; Swihart, M. T.; Prasad, P. N.; Walsh, T. R.; Knecht, M. R. Comparative Study of Materials-Binding Peptide Interactions with Gold and Silver Surfaces and Nanostructures: A Thermodynamic Basis for Biological Selectivity of Inorganic Materials *Chem. Mater.,* **2014,** *26*, 4960-4969, 10.1021/cm501529u

(17) Raut, V. P.; Agashe, M. A.; Stuart, S. J.; Latour, R. A. Molecular Dynamics Simulations of Peptide–Surface Interactions *Langmuir,* **2005,** *21*, 1629-1639, 10.1021/la047807f

(18) Latour, R. A. Molecular Simulation of Protein-Surface Interactions: Benefits, Problems, Solutions, and Future Directions (Review) *Biointerfaces,* **2008,** *3*, FC2-FC12, 10.1116/1.2965132

(19) Zin, M. T.; Ma, H.; Sarikaya, M.; Jen, A. K. Y. Assembly of Gold Nanoparticles Using Genetically Engineered Polypeptides *Small,* **2005,** *1*, 698-702, 10.1002/smll.200400164

(20) Hoefling, M.; Iori, F.; Corni, S.; Gottschalk, K.-E. Interaction of Amino Acids with the Au(111) Surface: Adsorption Free Energies from Molecular Dynamics Simulations *Langmuir,* **2010,** *26*, 8347-8351, 10.1021/la904765u

(21) Heinz, H.; Farmer, B. L.; Pandey, R. B.; Slocik, J. M.; Patnaik, S. S.; Pachter, R.; Naik, R. R. Nature of Molecular Interactions of Peptides with Gold, Palladium, and Pd–Au Bimetal Surfaces in Aqueous Solution *J. Am. Chem. Soc.,* **2009,** *131*, 9704-9714, 10.1021/ja900531f

(22) Heinz, H. Computational Screening of Biomolecular Adsorption and Self-Assembly on Nanoscale Surfaces *J. Comput. Chem.,* **2010,** *31*, 1564-1568, 10.1002/jcc.21421

(23) Friddle, R. W.; Battle, K.; Trubetskoy, V.; Tao, J.; Salter, E. A.; Moradian-Oldak, J.; De Yoreo, J. J.; Wierzbicki, A. Single-Molecule Determination of the Face-Specific Adsorption of

Amelogenin's C-Terminus on Hydroxyapatite *Angew. Chem. Int. Ed.,* **2011,** *50*, 7541-7545, 10.1002/anie.201100181

(24) Mijajlovic, M.; Penna, M. J.; Biggs, M. J. Free Energy of Adsorption for a Peptide at a Liquid/Solid Interface Via Nonequilibrium Molecular Dynamics *Langmuir,* **2013,** *29*, 2919-2926, 10.1021/la3047966

(25) Jarzynski, C. Nonequilibrium Equality for Free Energy Differences *Phys. Rev. Lett.,* **1997,** *78*, 2690-2693, 10.1103/PhysRevLett.78.2690

(26) Jarzynski, C. Equilibrium Free-Energy Differences from Nonequilibrium Measurements: A Master-Equation Approach *Physical Review E,* **1997,** *56*, 5018-5035, 10.1103/PhysRevE.56.5018

(27) Isralewitz, B.; Gao, M.; Schulten, K. Steered Molecular Dynamics and Mechanical Functions of Proteins *Curr. Opin. Struct. Biol.,* **2001,** *11*, 224-230, 10.1016/S0959-440X(00)00194-9

(28) Kulp Iii, J. L.; Sarikaya, M.; Spencer Evans, J. Molecular Characterization of a Prokaryotic Polypeptide Sequence That Catalyzes Au Crystal Formation *J. Mater. Chem.,* **2004,** *14*, 2325-2332, 10.1039/B401260G

(29) Kalé, L.; Skeel, R.; Bhandarkar, M.; Brunner, R.; Gursoy, A.; Krawetz, N.; Phillips, J.; Shinozaki, A.; Varadarajan, K.; Schulten, K. Namd2: Greater Scalability for Parallel Molecular Dynamics *J. Comput. Phys.,* **1999,** *151*, 283-312, 10.1006/jcph.1999.6201

(30) Heinz, H.; Vaia, R. A.; Farmer, B. L.; Naik, R. R. Accurate Simulation of Surfaces and Interfaces of Face-Centered Cubic Metals Using 12–6 and 9–6 Lennard-Jones Potentials *J. Phys. Chem. C,* **2008,** *112*, 17281-17290, 10.1021/jp801931d

(31) MacKerell, A. D.; Bashford, D.; Bellott, M.; Dunbrack, R. L.; Evanseck, J. D.; Field, M. J.; Fischer, S.; Gao, J.; Guo, H.; Ha, S.; et al. M. All-Atom Empirical Potential for Molecular Modeling and Dynamics Studies of Proteins *J. Phys. Chem. B,* **1998,** *102*, 3586-3616, 10.1021/jp973084f

(32) Price, D. J.; Brooks Iii, C. L. A Modified Tip3p Water Potential for Simulation with Ewald Summation *J. Chem. Phys.,* **2004,** *121*, 10096-10103, 10.1063/1.1808117

(33) Feng, J.; Pandey, R. B.; Berry, R. J.; Farmer, B. L.; Naik, R. R.; Heinz, H. Adsorption Mechanism of Single Amino Acid and Surfactant Molecules to Au {111} Surfaces in Aqueous Solution: Design Rules for Metal-Binding Molecules *Soft Matter,* **2011,** *7*, 2113-2120, 10.1039/C0SM01118E

(34) Park, S.; Khalili-Araghi, F.; Tajkhorshid, E.; Schulten, K. Free Energy Calculation from Steered Molecular Dynamics Simulations Using Jarzynski's Equality *J. Chem. Phys.,* **2003,** *119*, 3559-3566, 10.1063/1.1590311